Water-Catalyzed Dehalogenation Reactions of Isobromoform and Its Reaction Products

Wai Ming Kwok, Cunyuan Zhao, Yun-Liang Li, Xiangguo Guan, Dongqi Wang, and David Lee Phillips*

Contribution from the Department of Chemistry, The University of Hong Kong, Pokfulam Road, Hong Kong S.A.R., P. R. China

Received October 14, 2003; E-mail: phillips@hkucc.hku.hk

Abstract: A combined experimental and theoretical study of the photochemistry of $CHBr_3$ in pure water and in acetonitrile/water mixed solvents is reported that elucidates the reactions and mechanisms responsible for the photochemical conversion of the halogen atoms in $CHBr_3$ into three bromide ions in water solution. Ultraviolet excitation at 240 nm of $CHBr_3$ (9×10^{-5} M) in water resulted in almost complete conversion into 3HBr leaving groups and CO (major product) and HCOOH (minor product) molecules. Picosecond time-resolved resonance Raman (ps-TR^3) experiments and ab initio calculations indicate that the water-catalyzed O−H insertion/HBr elimination reaction of isobromoform and subsequent reactions of its products are responsible for the production of the final products observed following ultraviolet excitation of $CHBr_3$ in water. These results have important implications for the phase-dependent behavior of polyhalomethane photochemistry and chemistry in water-solvated environments as compared to gas-phase reactions. The dissociation reaction of HBr into H$^+$ and Br$^-$ ions is the driving force for several O−H insertion and HBr elimination reactions and allows O−H and C−H bonds to be cleaved more easily than in the absence of water molecules. This water-catalysis by solvation of a leaving group and its dissociation into ions (e.g., H$^+$ and Br$^-$ in the examples investigated here) may occur for a wide range of chemical reactions taking place in water-solvated environments.

Introduction

Polyhalomethanes such as CH_2I_2, $CHBr_3$, $CFCl_3$, and others have been observed in the natural environment and are important sources of reactive halogens in the atmosphere that have been linked to ozone depletion in the troposphere and/or the stratosphere.[1-11] Halogen activation processes in the natural environment[12-22] and the role of polyhalomethanes such as CH_2I_2 in the formation of iodine aerosols in the atmosphere[23]

have been areas of intense recent interest. In addition, photochemical processes of water treatment have used polyhalomethanes and other halogenated organic compounds to study and better understand the dehalogenation and decomposition of these types of compounds in water to design and improve photocatalysts for water treatment.[24,25]

Bromoform is the most abundant source of organic bromine in the ocean and atmosphere, and this makes it an attractive polyhalomethane to study.[1,26] Ultraviolet excitation with 253.7 nm light (from a Hg lamp) of low concentrations ($<10^{-6}$ M) of $CHBr_3$, $CHBr_2Cl$, and $CHCl_2Br$ in aqueous solution led to complete conversion of the halogens into halide ions (bromide and/or chloride) with similar photoquantum yields of about 0.43.[24] C−Br bond cleavage for the $CHBr_3$ molecule and the $CHBr_2$ radical in the gas phase has been estimated to require 63.8 and 73.6 kcal/mol of energy, respectively.[27] The 253.7 nm

(1) Wayne, R. P. *Chemistry of Atmospheres*, 3rd ed.; Oxford University Press: Oxford, U. K., 2000.
(2) Molina, M. J.; Rowland, F. S. *Nature* **1974**, *249*, 810−812.
(3) Molina, M. J.; et al. *Science* **1987**, *238*, 1253−1257.
(4) Class, Th.; Ballschmiter, K. *J. Atmos. Chem.* **1988**, *6*, 35−46.
(5) Klick, S.; Abrahamsson, K. *J. Geophys. Res.* **1992**, *97*, 12683−12687.
(6) Heumann, K. G. *Anal. Chim. Acta* **1993**, *283*, 230−245.
(7) Moore, R. M.; Webb, M.; Tokarczyk, R.; Wever, R. *J. Geophys. Res.-Oceans* **1996**, *101*, No. C9, 20899−20908.
(8) McElroy, C. T.; McLinden, C. A.; McConnell, J. C. *Nature* **1999**, *397*, 338−341.
(9) Mössinger, J. C.; Shallcross, D. E.; Cox, R. A. *J. Chem. Soc., Faraday Trans.* **1998**, *94*, 1391−1396.
(10) Carpenter, L. J.; Sturges, W. T.; Penkett, S. A.; Liss, P. S. *J. Geophys. Res.-Atmos.* **1999**, *104*, 1679−1689.
(11) Alicke, B.; Hebestreit, K.; Stutz, J.; Platt, U. *Nature* **1999**, *397*, 572−573.
(12) Fan, S. M.; Jacob, D. J. *Nature* **1992**, *359*, 522−524.
(13) Mozurkewich, M. *J. Geophys. Res.* **1995**, *100*, D7, 14199−14207.
(14) Vogt, R.; Crutzen, P. J.; Sander, R. *Nature* **1996**, *383*, 327−330.
(15) Sander, R.; Crutzen, P. J. *J. Geophys. Res.* **1996**, *101*, D4, 9121−9138.
(16) Oum, K. W.; Lakin, M. J.; DeHaan, D. O.; Brauers, T.; Finalyson-Pitts, B. J. *Science* **1998**, *279*, 74−77.
(17) McElroy, C. T.; McLinden, C. A.; McConnell, J. C. *Nature* **1999**, *397*, 338−341.
(18) Vogt, R.; Sander, R.; Glasow, R. V.; Crutzen, P. J. *J. Atmos. Chem.* **1999**, *32*, 375−395.
(19) Behnke, W.; Elend, M.; Krüger, U.; Zetzsch, C. *J. Atmos. Chem.* **1999**, *34*, 87−99.
(20) Knipping, E. M.; Lakin, M. J.; Foster, K. L.; Jungwirth, P.; Tobias, D. J.; Gerber, R. B.; Dabdub, D.; Finlayson-Pitts, B. J. *Science* **2000**, *288*, 301−306.
(21) Finlayson-Pitts, B. J.; Hemminger, J. C. *J. Phys. Chem. A* **2000**, *104*, 11463−11477.
(22) Foster, K. L.; Plastridge, R. A.; Bottenheim, J. W.; Shepson, P. B.; Finlayson-Pitts, B. J.; Spicer, C. W. *Science* **2001**, *291*, 471−474.
(23) O'Dowd, C. D.; Jimenez, J. L.; Bahreini, R.; Plagan, R. C.; Seinfeld, J. H.; Hamerl, K.; Pirjola, L.; Kulmala, M.; Jennings, S. G.; Hoffmann, T. *Nature* **2002**, *417*, 632−636.
(24) Nicole, I.; de Laat, J.; Dore, M.; Duguet, J. P.; Suty, H. *Environ. Technol.* **1991**, *12*, 21−31.
(25) Legrini, O.; Oliveros, E.; Bruan, A. M. *Chem. Rev.* **1993**, *93*, 671−698.
(26) Quack, B.; Wallace, D. W. R. *Global Biogeochem. Cycles* **2003**, *17*, Art. No. 1023.

photon has about 113 kcal/mol of energy and is thus only likely to break one carbon–halogen bond in the $CHBr_3$, $CHBr_2Cl$, and $CHCl_2Br$ molecules following 253.7 nm excitation. How does the 253.7 nm photolysis of low concentrations of $CHBr_3$, $CHBr_2Cl$, and $CHCl_2Br$ in water lead to complete conversion of the halogen atoms into bromide and/or chloride ion products, and where does the energy come from to break all three carbon–halogen bonds? Here, we present a combined experimental and theoretical study of the photochemistry of $CHBr_3$ in pure water and in acetonitrile/water mixed solvents. This work elucidates the reactions and mechanisms responsible for the photochemical conversion of the halogen atoms in $CHBr_3$ into three bromide ions in water solution.

Experimental and Computational Methods

Photochemistry and Product Analysis Experiments. Ultraviolet/Visible Absorption and pH Measurements after Photolysis of $CHBr_3$ in Water. Commercially available $CHBr_3$ (99%) and deionized water were used to prepare 500 mL sample solutions of about 9×10^{-5} M $CHBr_3$ in water. The sample solution was put in a 10 cm laser path-length glass holder with quartz windows and was excited by 3 mJ of 240 nm unfocused laser beam from the first anti-Stokes hydrogen Raman shifted laser line of the fourth harmonic of a nanosecond-Nd: YAG laser in the photolysis experiments. The absorption spectra for the photolyzed samples were acquired by employing a 1 cm UV grade cell and a Perkin-Elmer Lambda 19 UV/vis spectrometer. The pH of the photolyzed samples was measured by using a ThermoOrion 420A pH meter equipped with a 8102BN combination pH electrode. The pH electrode was calibrated with 7.00 pH and 4.01 pH buffer solutions.

^{13}C NMR Measurements after 240 nm Photolysis of $CHBr_3$ in Water. Commercially available $^{13}CHBr_3$ (Aldrich) and D_2O (99.9% D) solvent were used to prepare ~20 mM sample solutions which were placed in a UV-grade airtight NMR tube for the photolysis experiments. ^{13}C NMR spectra were acquired using a Bruker Advance 400 DPX spectrometer at room temperature. An initial ^{13}C NMR spectrum was obtained for the sample before photolysis, and additional spectra were obtained after varying times following excitation by the 240 nm unfocused laser beam until all of the $^{13}CHBr_3$ sample was photolyzed as determined by the decrease in its ^{13}C NMR band at ~12 ppm referenced to the TMS band that was set as 0 ppm.

Infrared (IR) Absorption Measurements after 240 nm Photolysis of $CHBr_3$ in Water. The evolution of gas was observed in both of the photochemistry experiments described in parts 1 and 2 above. This gas was collected and introduced into a 10 cm path-length IR gas cell equipped with KBr windows. IR spectra of the gas obtained after photolysis of $CHBr_3$ in water were obtained using a Bio-Rad FTS 165 spectrometer.

We attempted to estimate the photoquantum yield for the photolysis reaction of $CHBr_3$ in water to produce $3Br^-$ (e.g., 3HBr that dissociate to $3H^+$ and $3Br^-$ in water). The same setup as for the UV/vis absorption measurements described above and a laser power meter to measure the laser beam exciting the sample solution were used to make the experimental measurements needed to estimate the photoquantum yield. The equations given in the Supporting Information were used to find the estimate of the photoquantum yield for production of the 3HBr leaving groups.

Picosecond Time-Resolved Resonance Raman (ps-TR^3) Experiments. A femtosecond mode-locked Ti:Sapphire laser (Spectra-Physics, Tsunami) pumped by the second harmonic from a Nd:YVO$_4$ laser (Spectra-Physics, Millennia V) was employed as the seed beam for an amplified laser system. A picosecond mode regenerative amplifier

(Spectra-Physics, Spitfire) pumped by the second harmonic from a Nd: YLF laser (Spectra-Physics, Evolution X) amplified the seed laser beam, and the output from the regenerative amplifier (800 nm, 1ps, 1 kHz) was frequency doubled and tripled by KDP crystals to generate the probe (400 nm) and pump (267 nm) laser sources, respectively. The time zero delay between the pump and probe laser beams in the TR^3 experiments was found by using fluorescence depletion of *trans*-stilbene. The time zero was ascertained by varying the optical delay between the pump and probe beams to a position where the depletion of the stilbene fluorescence was halfway to the maximum fluorescence depletion by the probe laser. The accuracy of the time zero measurement was estimated to be ±0.5 ps, and a typical cross-correlation time between the pump and probe pulses was also measured by the fluorescence depletion method and determined to be about 1.5 ps (fwhm). So as to employ the laser beams more effectively in the TR^3 experiments and taking into account that the rotational reorientation dynamics are much faster than the dynamics investigated in this study, parallel polarization of the pump and probe laser beams was employed rather than the magic angle polarization. The pump and probe pulses were loosely focused onto a thin film stream (thickness ~500 μm) of the sample solution where typical pulse energies and spot sizes at the sample for the pump beam were 15 μJ and 250 μm and for the probe beam were 8 μJ and 150 μm. A backscattering geometry using an ellipsoidal mirror with $f/1.4$ was employed to collect the Raman scattered light and image the light onto the entrance slit of a 0.5 m spectrograph. The 1200 groove/mm ruled grating blazed at 250 nm of the spectrograph dispersed the Raman scattered light onto a liquid nitrogen cooled CCD detector mounted on the exit port of the spectrograph.

Each spectrum shown here was obtained from subtraction of scaled probe-before-pump and scaled net solvent measurements from a pump–probe spectrum to delete $CHBr_3$ ground-state Raman bands and residual solvent Raman bands, respectively. The known Raman shifts of the solvent Raman bands were used to calibrate the spectra with an estimated accuracy of ±5 cm^{-1} in absolute frequency. Commercially available 99% $CHBr_3$ and spectroscopic grade acetonitrile solvent were used without further purification to make half-liter volume $CHBr_3$ (8×10^{-2} mol dm^{-3}) samples prepared in acetonitrile and acetonitrile/water (0.2%, 1%, 2%, 5%) mixed solvents. During the experimental trials, the samples showed less than a few percent degradation as determined from the UV absorption spectra obtained before and after the TR^3 measurement.

Ab Initio Calculations. The second-order Møller–Plesset perturbation theory (MP2) was employed to examine the water-assisted O–H insertion reactions of isobromoform ($BrCHBr–Br$) + nH_2O → $CHBr_2(OH)$ + HBr + $(n-1)H_2O$ (where $n = 1,2,3$), and the decomposition reactions of $CHBr_2(OH)$ + nH_2O → HBrCO + nH_2O + HBr ($n = 0,1,2,3,4$) and HBrCO + nH_2O → CO + HBr + nH_2O ($n = 0,1,2,...,4$). Both the geometry optimization and the frequency calculations were done with the 6-31G* basis set for C, H, O, and Br atoms. MP2 calculations using a 6-311++G** basis set were also done to find the optimized geometry, vibrational frequencies, and relative Raman intensities for the $CHBr_2OH$ molecule. All of the calculations made use of the Gaussian 98W program suite.[28] Cartesian coordinates, total energies, and selected output from the calculations for all of the calculated structures shown in Figures 4–6 are given in the Supporting

(27) McGivern, W. S.; Sorkhabi, O.; Suits, A. G.; Derecskei-Kovacs, A.; North, S. W. *J. Phys. Chem. A* **2000**, *104*, 10085–10091.

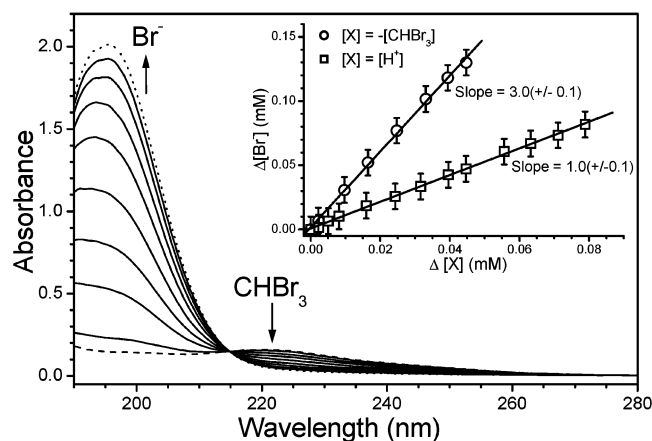(28) Frisch, M. J.; Trucks, G. W.; Schlegel, H. B.; Scuseria, G. E.; Robb, M. A.; Cheeseman, J. R.; Zakrzewski, V. G.; Montgomery, J. A., Jr.; Stratmann, R. E.; Burant, J. C.; Dapprich, S.; Millam, J. M.; Daniels, A. D.; Kudin, K. N.; Strain, M. C.; Farkas, O.; Tomasi, J.; Barone, V.; Cossi, M.; Cammi, R.; Mennucci, B.; Pomelli, C.; Adamo, C.; Clifford, S.; Ochterski, J.; Petersson, G. A.; Ayala, P. Y.; Cui, Q.; Morokuma, K.; Malick, D. K.; Rabuck, A. D.; Raghavachari, K.; Foresman, J. B.; Cioslowski, J.; Ortiz, J. V.; Baboul, A. G.; Stefanov, B. B.; Liu, G.; Liashenko, A.; Piskorz, P.; Komaromi, I.; Gomperts, R.; Martin, R. L.; Fox, D. J.; Keith, T.; Al-Laham, M. A.; Peng, C. Y.; Nanayakkara, A.; Gonzalez, C.; Challacombe, M.; Gill, P. M. W.; Johnson, B.; Chen, W.; Wong, M. W.; Andres, J. L.; Gonzalez, C.; Head-Gordon, M.; Replogle, E. S.; Pople, J. A. *Gaussian 98*; Gaussian, Inc.: Pittsburgh, PA, 1998.

Figure 1. Absorption spectra obtained after 240 nm photolysis of 9×10^{-5} M CHBr$_3$ in water. The parent CHBr$_3$ band at $\sim$223 nm decreases in intensity, and a new band at $\sim$190 nm due to Br$^-$ grows in with an isosbestic point at $\sim$215 nm with the parent band. The inset presents plots of Δ[Br$^-$] versus $-\Delta$[CHBr$_3$] (○) and Δ[H$^+$] (□), respectively, derived from the absorption spectra and pH measurements acquired during the same photochemistry experiments. The lines are linear best-fits to the data.

Information. IRC (intrinsic reaction coordinate) calculations were done to confirm the transition state connected the appropriate reactants and products.[29]

The stabilization energies from separated reactants to reactant complexes may be overestimated noticeably due to basis set superposition error (BSSE) effects, and the counterpoise (CP) method is often used to make a correction. We note that a study on water dimers found estimates of the effects of BSSE by the CP method may not lead to better results because they do not provide quantitative information about the basis set deficiencies.[30] In addition, the use of larger basis sets where the CP correction is small does not guarantee accurate results, and when smaller basis sets are employed, the inclusion of the CP correction does not systematically improve the accuracy of the calculations.[31] In our present study, we are primarily interested in the relative energies from the reactant complexes to their transition states which have the same number of basis functions, and in this case the effect from BSSE is expected to be small or canceled noticeably. This and the ambiguity in the benefits of using BSSE corrections led us not to use the BSSE corrections in the present study.

Results

Observation of Efficient CHBr$_3$ Dehalogenation after Ultraviolet Photolysis in Water. Figure 1 shows ultraviolet/visible (UV/vis) absorption spectra obtained after 240 nm photolysis of CHBr$_3$ (9×10^{-5} M) in water. The absorption bands in the 220–230 nm region due to CHBr$_3$ decrease in intensity, while a new band at about 190 nm due to Br$^-$ increases in intensity for increasing photolysis times. The clear isosbestic point at $\sim$215 nm indicates Br$^-$ is directly produced from the CHBr$_3$ parent molecule. The pH of the sample solutions was measured at the same time each UV/vis spectrum was acquired during the photolysis experiments depicted in Figure 1. The inset of Figure 1 shows a plot of Δ[Br$^-$] versus $-\Delta$[CHBr$_3$] derived from the photolysis experiments and reveals the increase of

(29) (a) Gonzalez, C.; Schlegel, H. B. *J. Chem. Phys.* **1989**, *90*, 2154–2161; (b) *J. Phys. Chem.* **1990**, *94*, 5523–5527.
(30) Frisch, M. J.; Del Bene, J. E.; Binkley, J. S.; Schaefer, H. F., III. *J. Chem. Phys.* **1986**, *84*, 2279.
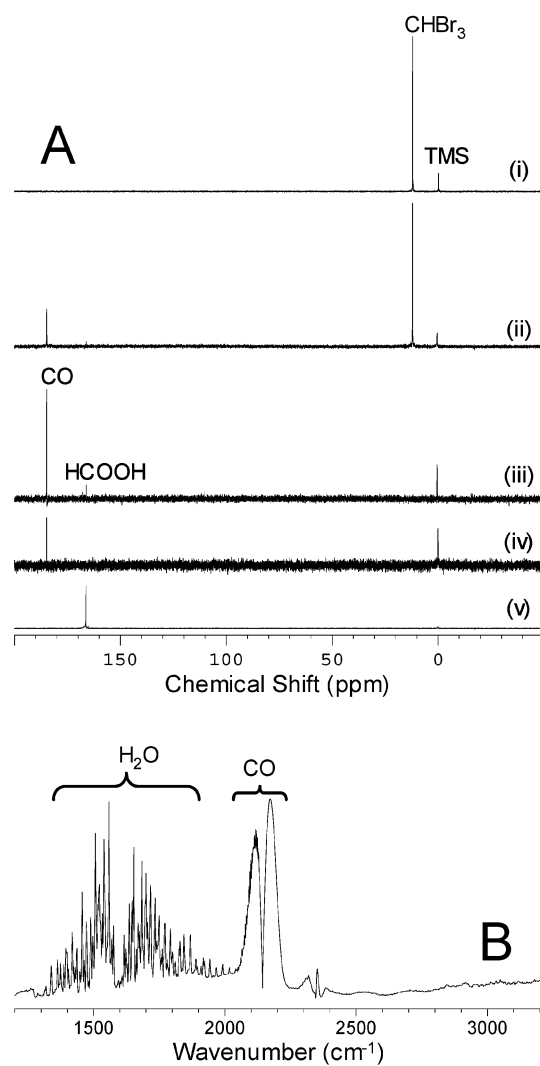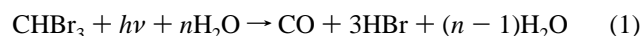(31) Schwenke, D. W.; Truhlar, D. G. *J. Chem. Phys.* **1985**, *82*, 2418.

Figure 2. (A) ^{13}C NMR spectra acquired before (i), during (ii), and after complete photolysis (iii) of ^{13}CHBr$_3$ in D$_2$O solvent. Photolysis converts the parent ^{13}CHBr$_3$ band at 12 ppm into new photoproduct bands at 185 ppm and 166 ppm assigned to CO and HCOOH, respectively. The identities of the photoproduct bands were confirmed by ^{13}C NMR spectra of authentic samples of CO (iv) and HCOOH (v). (B) Infrared spectrum of gas produced during photolysis of CHBr$_3$ in water.

[Br$^-$] versus the decrease in [CHBr$_3$] has a linear relationship with a slope of about 3. A plot of the changes in the [H$^+$] concentrations derived from the pH measurements was plotted versus the changes in the [Br$^-$] concentrations (inset of Figure 1), and this exhibits a linear relationship with a slope of about 1. These results for the UV/vis and pH photochemistry experiments (in Figure 1) indicate that ultraviolet photolysis of CHBr$_3$ in water at low concentrations ($<10^{-4}$ M) releases 3H$^+$ and 3Br$^-$ products (e.g., 3HBr leaving groups that dissociate to 3H$^+$ and 3Br$^-$ in water solvent).

To determine the fate of the carbon atom from the CHBr$_3$ parent molecule following 240 nm photolysis, a carbon-13 labeled sample of CHBr$_3$ was used to repeat the 240 nm photolysis experiments in water. ^{13}C NMR spectra were obtained before, during, and after complete photolysis of ^{13}CHBr$_3$ in D$_2$O solvent (shown in Figure 2A-i–iii) in an airtight NMR tube. The parent ^{13}CHBr$_3$ band at 12 ppm decreases in intensity, and a new major photoproduct band appears at 185 nm accompanied by a minor photoproduct band at 166 ppm (both relative to the
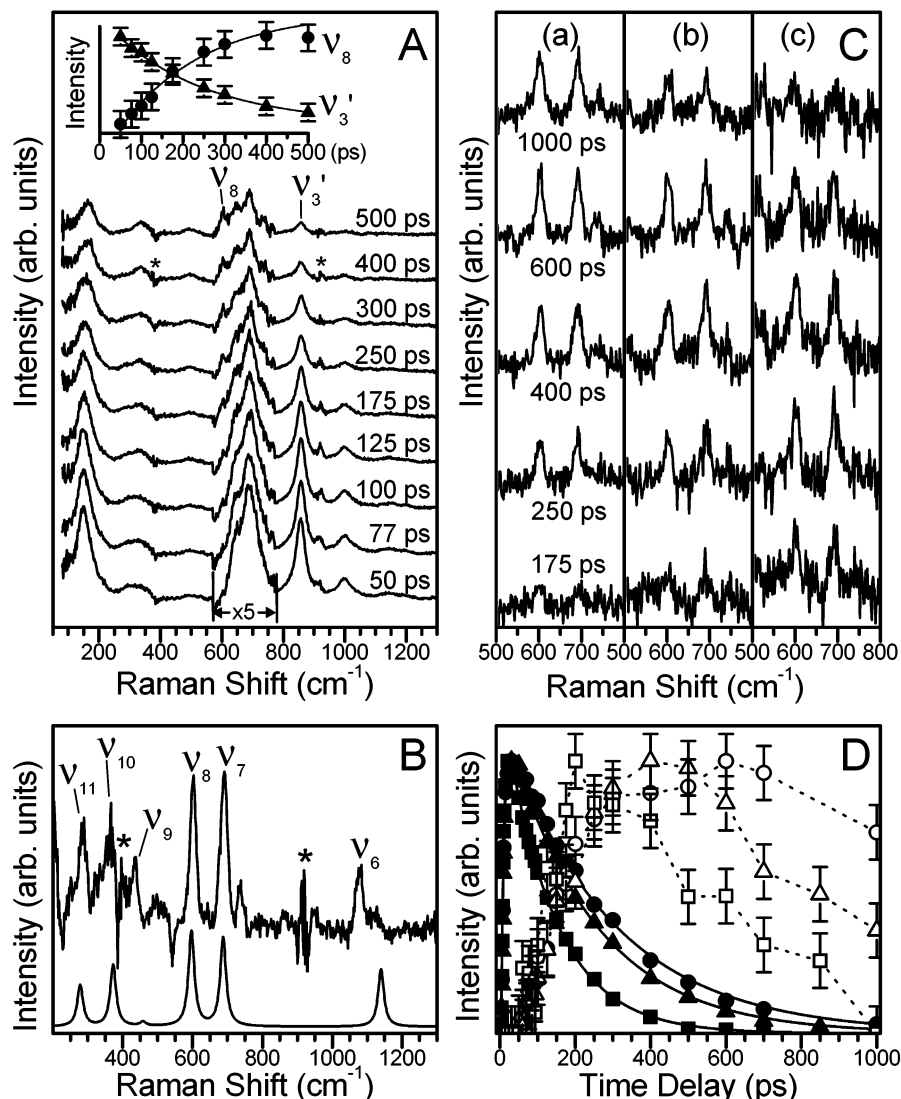
Figure 3. (A) Ps-TR^3 spectra acquired after 267 nm photolysis of CHBr$_3$ in acetonitrile/0.2% water mixed solvent at selected delay times between the pump and probe pulses. The inset displays a plot of the intensities of the ν_3' isobromoform (▲) and ν_8 CHBr$_2$OH (●) Raman bands as a function of delay time, and the solid lines are single-exponential decay and growth fits of the data, respectively. (B) Ps-TR^3 spectrum of CHBr$_2$OH photoproduct (top) found by subtracting an appropriately scaled 100 ps spectrum from the 500 ps spectrum shown in (A) (with a longer accumulation time) and comparison to MP2/6-311++G** calculated Raman spectra for CHBr$_2$OH. (C) Ps-TR^3 spectra of the largest CHBr$_2$OH Raman bands (ν_7 and ν_8) found as in (B) for selected delay times in acetonitrile/trace amounts of water (a), acetonitrile/0.2% water (b), and acetonitrile/1% water (c) mixed solvents. The asterisks mark solvent subtraction artifacts. (D) Plots of the isobromoform (solid points and lines) and CHBr$_2$OH (open points and dashed lines) Raman band intensities as a function of delay times in acetonitrile/trace amounts of water (circle), acetonitrile/0.2% water (triangle), acetonitrile/1% water (square) mixed solvents. Error bars are indicated for the weaker Raman band intensities of CHBr$_2$OH, while the error bars are much smaller and generally within the size of the data points shown for the more intense isobromoform Raman bands.

TMS reference band). After complete photolysis, the parent ^{13}CHBr$_3$ band has disappeared, and only the photoproduct bands at 185 and 166 ppm are left. Noticeable amounts of gas were formed during the preceding photochemistry experiments. This gas was collected, and an infrared spectrum was obtained (see Figure 2B). This spectrum shows large bands at 2116 and 2174 cm^{-1} due to CO. ^{13}C NMR spectra were obtained for authentic samples of CO and HCOOH and compared to the spectra obtained from the photochemistry experiments (Figure 2A-iv and v). This comparison clearly shows the characteristic 185 ppm major band and the 166 ppm minor band in the ^{13}C NMR spectra for the photoproducts are due to CO and HCOOH products, respectively.

Combining the preceding experimental photochemistry results suggests that ultraviolet photolysis of low concentrations ($<10^{-4}$ M) of CHBr$_3$ in water leads to the following overall reactions for the major and minor photoproduct channels:

major products

$$CHBr_3 + h\nu + nH_2O \rightarrow CO + 3HBr + (n-1)H_2O \quad (1)$$

minor products

$$CHBr_3 + h\nu + nH_2O \rightarrow HCOOH + 3HBr + (n-2)H_2O \quad (2)$$

The experimental results shown in Figures 1 and 2 indicate that the above reactions can convert almost all of the parent CHBr$_3$ compound under low concentration conditions into CO and 3HBr major products and some HCOOH and 3HBr minor
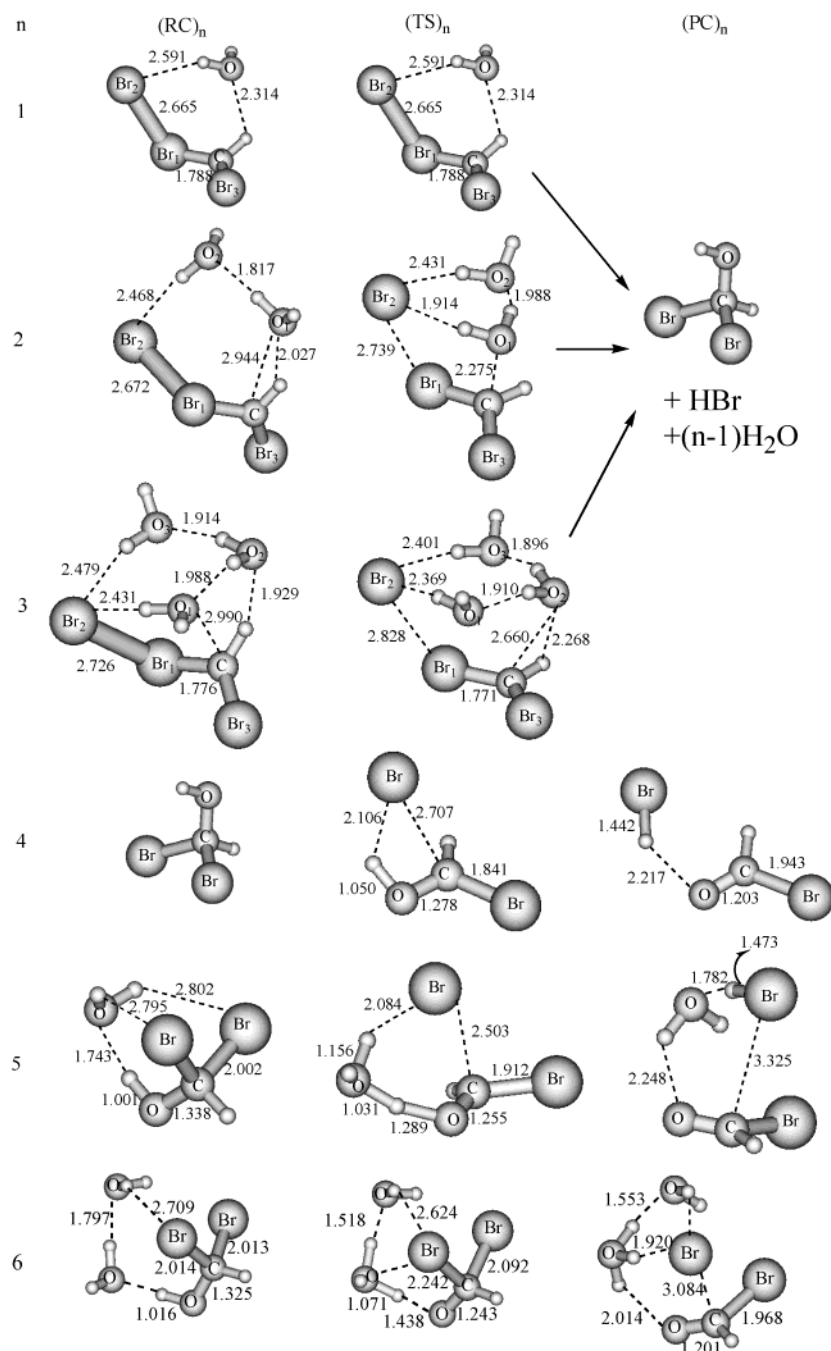
Figure 4. The optimized geometries for all of the reactants, reactant complexes, transition states, and product complexes obtained from the MP2/6-31G* computations are shown for the isobromoform + $nH_2O \rightarrow CHBr_2OH + HBr + (n-1)H_2O$, where $n = 1,2,3$ (associated with structures $(RC)_{1-3}$, $(TS)_{1-3}$, and $CHBr_2OH + (n-1)H_2O$), and $CHBr_2OH + nH_2O \rightarrow HBrCO + HBr + nH_2O$, where $n = 0,1,2$ (associated with structures $(RC)_{4-6}$, $(TS)_{4-6}$, and $(PC)_{4-6}$), reactions.

products with no other discernible products. The photoquantum yield for formation of 3HBr from reactions 1 and 2 was determined to be about 0.46 ± 0.1 from the disappearance of $CHBr_3$ and formation of 3HBr (see Supporting Information for more details). Thus, the overall photochemistry appears to be a fairly efficient process. The present experimental results are consistent with and in good agreement with previous studies that showed 253.7 nm excitation of $CHBr_3$ in water leads to complete conversion into bromide ions with a photolysis quantum yield of 0.43.[24]

Picosecond Time-Resolved Resonance Raman Spectra and Results. What species produced by ultraviolet photolysis of

$CHBr_3$ in water can lead to efficient reactions to produce CO and 3HBr major products accompanied by HCOOH and 3HBr minor products? Picosecond time-resolved resonance Raman (ps-TR[3]) experiments recently revealed that photolysis of CH_2I_2 in largely aqueous solutions leads to appreciable formation of an isodiiodomethane (CH_2I-I) photoproduct with its lifetime becoming shorter in mixed aqueous solvents as the amount of O−H bonds in the solvent system increases, suggesting that isodiiodomethane could be reacting with the H_2O solvent molecules.[32] Isodiiodomethane and other isopolyhalomethanes have been shown both theoretically and experimentally to be effective carbenoid species that can react with carbon double
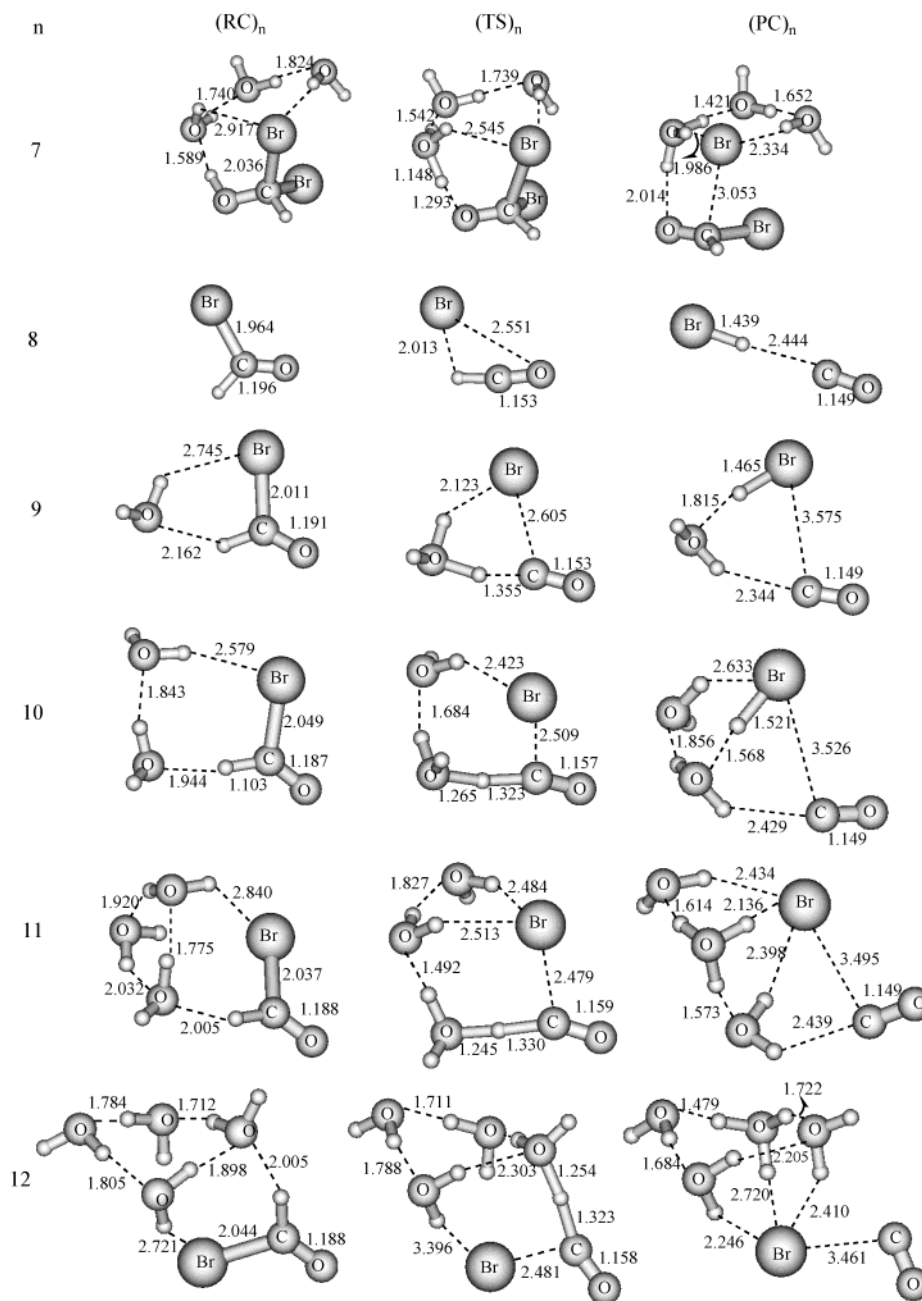
Figure 5. The optimized geometries for all of the reactants, reactant complexes, transition states, and product complexes obtained from the MP2/6-31G* computations are shown for the CHBr$_2$OH + nH$_2$O → HBrCO + HBr + nH$_2$O, where n = 3 (associated with structures (RC)$_7$, (TS)$_7$, and (PC)$_7$), and HBrCO + nH$_2$O → CO + HBr + nH$_2$O, where n = 0,1,2,3,4 (associated with structures (RC)$_{8-12}$, (TS)$_{8-12}$, and (PC)$_{8-12}$), reactions.

bonds to produce cyclopropanated products[33-40] in a manner similar to the reaction of singlet methylene with carbon double bonds.[35,36,41,42] Carbenes such as singlet methylene and dichlorocarbene (:CCl$_2$) can react with water via O–H insertion reactions to form CH$_3$OH and CHCl$_2$(OH) products, respectively,[43-50] similar to O–H insertion reactions of carbenes with alcohols.[51,52] Thus, one may expect that CH$_2$I–I and other

(32) Kwok, W. M.; Ma, C.; Parker, A. W.; Phillips, D.; Towrie, M.; Matousek, P.; Phillips, D. L. *J. Phys. Chem. A* **2003**, *107*, 2624–2628.
(33) Zheng, X.; Fang, W.-H.; Phillips, D. L. *J. Chem. Phys.* **2000**, *113*, 10934–10946.
(34) Zheng, X.; Lee, C. W.; Li, Y.-L.; Fang, W.-H.; Phillips, D. L. *J. Chem. Phys.* **2001**, *114*, 8347–8356.
(35) Phillips, D. L.; Fang, W.-H.; Zheng, X. *J. Am. Chem. Soc.* **2001**, *123*, 4197–4203.
(36) Phillips, D. L.; Fang, W.-H. *J. Org. Chem.* **2002**, *66*, 5890–5896.
(37) Li, Y.-L.; Leung, K. H.; Phillips, D. L. *J. Phys. Chem. A* **2001**, *105*, 10621–10625.
(38) Fang, W.-H.; Phillips, D. L.; Wang, D.; Li, Y.-L. *J. Org. Chem.* **2002**, *67*, 154–160.
(39) Li, Y.-L.; Chen, D. M.; Wang, D.; Phillips, D. L. *J. Org. Chem.* **2002**, *67*, 4228–4235.
(40) Li, Y.-L.; Wang, D.; Phillips, D. L. *J. Chem. Phys.* **2002**, *117*, 7931–7941.

(41) Zurawski, B.; Kutzelnigg, W. *J. Am. Chem. Soc.* **1978**, *100*, 2654–2659.
(42) Sakai, S. *Int. J. Quantum Chem.* **1998**, *70*, 291–302.
(43) Harding, L. B.; Schlegel, H. B.; Krishnan, R.; Pople, J. A. *J. Phys. Chem.* **1980**, *84*, 3394–3401.
(44) Pople, J. A.; Raghavachari, K.; Frisch, M. J.; Blinkley, J. B.; Schleyer, P. V. R. *J. Am. Chem. Soc.* **1983**, *105*, 6389–6398.
(45) Wesdemiotis, C.; Feng, R.; Danis, P. O.; Williams, E. R.; Lafferty, F. W. *J. Am. Chem. Soc.* **1986**, *108*, 5847–5853.
(46) Yates, B. F.; Bouma, W. J.; Radom, L. *J. Am. Chem. Soc.* **1987**, *109*, 2250–2263.
(47) Walch, S. P. *J. Chem. Phys.* **1993**, *98*, 3163–3178.
(48) Gonzalez, C.; Restrepo-Cossio, A.; Márquez, M.; Wiberg, K. B. *J. Am. Chem. Soc.* **1996**, *118*, 5408–5411.
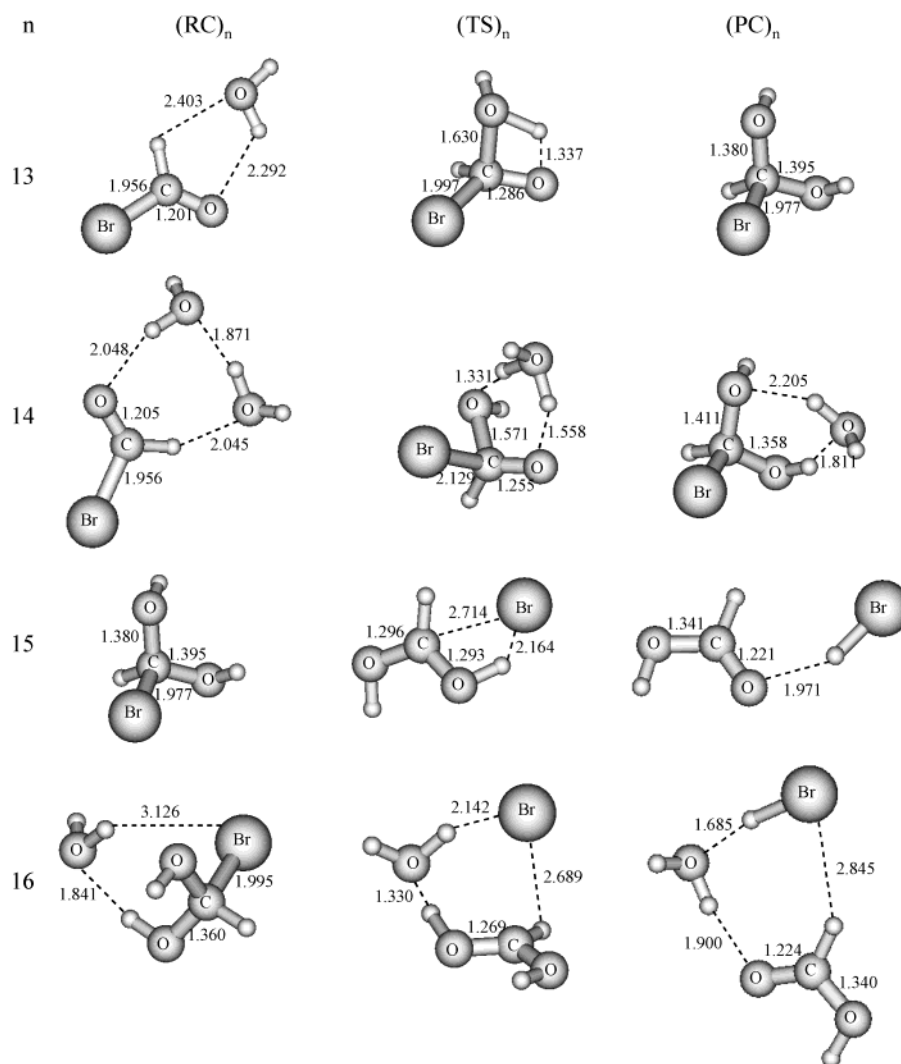
Figure 6. The optimized geometries for all of the reactants, reactant complexes, transition states, and product complexes obtained from the MP2/6-31G* computations are shown for the HBrCO + nH$_2$O → HBrCOH$_2$ + (n − 1)H$_2$O, where n = 1,2 (associated with structures (RC)$_{13-14}$, (TS)$_{13-14}$, and (PC)$_{13-14}$), and HBrCOH$_2$ + nH$_2$O → HCOOH + HBr + nH$_2$O, where n = 0,1 (associated with structures (RC)$_{15-16}$, (TS)$_{15-16}$, and (PC)$_{15-16}$), reactions.

isopolyhalomethanes could also react with water in a manner similar to that of carbenes.

Preliminary ab initio work showed that CH$_2$I−I was able to react with water via an O−H insertion reaction to produce CH$_2$I-(OH) and HI products.[53] This O−H insertion/HI elimination reaction was also found to be catalyzed by the presence of a second water molecule in a manner similar to the dichlorocarbene O−H insertion reactions with H$_2$O and 2H$_2$O.[53] These results for CH$_2$I−I suggest that isopolyhalomethane molecules are probably noticeably reactive with water and undergo O−H insertion/HX elimination reactions to produce a halogenated methanol product and HX leaving group. We recently directly observed the O−H insertion reaction of isobromoform with water to produce a CHBr$_2$(OH) product in an acetonitrile/0.2% water mixed solvent system using ps-TR^3 spectroscopy.[54] Here,

we report further ps-TR^3 experiments to examine how the isobromoform and CHBr$_2$(OH) species are affected by the concentration of water.

An overview of the ps-TR^3 spectra obtained in acetonitrile solvent with trace amounts of water, and acetonitrile with 0.2%, 1%, 2%, and 5% amounts of water, is given in Supporting Information Figures S1−S5. These spectra are similar to those observed previously in spectra obtained in acetonitrile/0.2% water mixed solvent,[54] and all show the isobromoform species is produced within several picoseconds and then vibrationally cooled on the 10−50 ps time-scale as has been found for isobromoform and other isopolyhalomethanes in ps-TR^3 experiments.[32,54−57] The assignments of the isobromoform Raman bands in the ps-TR^3 spectra in Figures S1−S5 and Figure 3A are in good agreement with those previously observed in ns-TR^3 spectra of isobromoform in cyclohexane solvent,[33] and

(49) Pliego, J. R., Jr.; De Almeida, W. B. *J. Phys. Chem.* **1996**, *100*, 12410−12413.
(50) Pliego, J. R., Jr.; De Almeida, W. B. *J. Phys. Chem. A* **1999**, *103*, 3904−3909.
(51) Moody, C. J.; Whitman, G. H. In *Reactive Intermediates*; Davies, S. G., Ed.; Oxford University Press: New York, 1992.
(52) Kirmse, W.; Meinert, T.; Moderelli, D. A.; Platz, M. S. *J. Am. Chem. Soc.* **1993**, *115*, 8918−8927.
(53) Li, Y.-L.; Zhao, C.; Kwok, W. M.; Guan, X.; Zuo, P.; Phillips, D. L. *J. Chem. Phys.* **2003**, *119*, 4671−4681.

(54) Kwok, W. M.; Zhao, C.; Li, Y.-L.; Guan, X.; Phillips, D. L. *J. Chem. Phys.*, in press.
(55) Kwok, W. M.; Ma, C.; Parker, A. W.; Phillips, D.; Towrie, M.; Matousek, P.; Phillips, D. L. *J. Chem. Phys.* **2000**, *113*, 7471−7478.
(56) Kwok, W. M.; Ma, C.; Parker, A. W.; Phillips, D.; Towrie, M.; Matousek, P.; Zheng, X.; Phillips, D. L. *J. Chem. Phys.* **2001**, *114*, 7536−7543.
(57) Kwok, W. M.; Ma, C.; Parker, A. W.; Phillips, D.; Towrie, M.; Matousek, P.; Phillips, D. L. *Chem. Phys. Lett.* **2001**, *341*, 292−298.

Table 1. Comparison of Experimental and Calculated Vibrational Frequencies (in cm^{-1}) for the CHBr$_2$OH Photoproduct Species (See the Text for More Details on the Description of the MP2/ 6-311++G** ab Initio Calculations)

Raman bands of second species in acet./0.2% of H$_2$O 500 ps spectrum Ps-TR^3 expt. 400 nm probe	CHBr$_2$OH MP2 calc. 6-311++G**	possible qualitative description for the vibrational modes
	A′ ν_1 3836	O–H stretch
	ν_2 3220	C–H stretch
	ν_3 1419	O–H + C–H bend (asym.)
	ν_4 1249	O–H + C–H bend (sym.) + C–O str.
	ν_5 1219	C–H bend
1078	$_6\nu$ **1140**	C–O stretch
690	$_7\nu$ **688**	Br–C–Br asymmetric stretch
601	$_8\nu$ **597**	Br–C–Br symmetric stretch
433	$_9\nu$ **458**	O–H bend
361	$_1\nu_0$ **373**	C–BrBrH umbrella
284	$_1\nu_1$ **278**	Br–C–Br stretch/bend
	ν_{12} 175	Br–C–Br in plane bend or scissor

Table S1 provides details of the vibrational assignments. Figure 3A presents ps-TR^3 spectra acquired at selected times after photolysis of CHBr$_3$ in acetonitrile/0.2% water solvent. The Raman bands of isobromoform (the major band ν_3' is highlighted in Figure 3A) decay, and new Raman bands assigned to a CHBr$_2$(OH) reaction product (the major band ν_8 is highlighted in Figure 3A) are formed. The formation of these new Raman bands is directly correlated to the decay of the isobromoform bands (see inset of Figure 3A that compares the decay of the ν_3' isobromoform band intensity to that of the growth of the ν_8 CHBr$_2$(OH) band intensity) and indicates the new Raman bands are a reaction product of isobromoform. The lifetime of isobromoform strongly depends on the concentration of H$_2$O. The lifetimes vary between 283, 225, 133, 89, and 46 ps in acetonitrile/trace amounts, 0.2%, 1%, 2%, and 5% of H$_2$O mixed solvents, respectively (see plots of the ν_3' isobromoform band intensities in Figure 3D and ps-TR^3 spectra in Figures S1–S5 of the Supporting Information). This indicates isobromoform is reacting with H$_2$O to make the reaction product observed correlate with its decay. This is further supported by the observation that, as the isobromoform Raman band intensity decays faster as the water concentration increases, the second species appearance grows in faster and directly correlates with the reaction of isobromoform with water. Figure 3B compares a ps-TR^3 spectrum of the new reaction product found by subtracting an appropriately scaled 100 ps spectrum (Raman bands mainly due to isobromoform) from the 500 ps spectrum (Raman bands due to both isobromoform and its reaction product) of Figure 3A with the Raman spectrum computed from ab initio calculations for the CHBr$_2$(OH) molecule. Inspection of Figure 3B shows there is good agreement between the experimental ps-TR^3 spectrum for the reaction product by itself and the ab initio calculated Raman spectrum for the CHBr$_2$-(OH) molecule. This identifies CHBr$_2$(OH) as the reaction product species produced from the isobromoform O–H insertion reaction with water (see Table 1 for details of the vibrational band assignments).

Figure 3C presents selected ps-TR^3 spectra for the CHBr$_2$-(OH) product found by subtracting an appropriately scaled 100 or 50 ps spectrum from spectra acquired at later times for CHBr$_3$ photolysis in acetonitrile/trace amounts, 0.2%, and 1% mixed

solvents. Figure 3C shows the 500–800 cm^{-1} region where the larger ν_8 and ν_7 vibrational modes of CHBr$_2$(OH) appear. Figure 3D presents plots of the Raman intensity of the CHBr$_2$(OH) product as a function of time-delay for the mixed solvent systems with varying concentrations of water. The CHBr$_2$(OH) product bands in Figure 3C decay substantially faster at a high concentration of water, and this indicates that the CHBr$_2$(OH) product undergoes further reaction with water to produce another reaction product. The reactions of isobromoform and CHBr$_2$-(OH) with water molecules were explored by systematically varying the number of water molecules in the reaction system using ab initio calculations as described in the next section.

Building Water-Catalyzed O–H Insertion and HBr Elimination Reactions One Molecule at a Time. Ab initio calculations (MP2/6-31G*) were done to study the isobromoform + nH$_2$O → CHBr$_2$OH + HBr + (n − 1)H$_2$O where n = 1,2,3, CHBr$_2$OH + nH$_2$O → HBrCO + HBr + nH$_2$O where n = 0,1,2,3, and HBrCO + nH$_2$O → CO + HBr + nH$_2$O where n = 0,1,2,3,4 reactions. The optimized geometries for all of the reactants, reactant complexes, transition states, and product complexes obtained from the MP2 computations are shown in Figures 4–6. IRC calculations were done to confirm the transition states connected the appropriate reactants and products.[29] The relative energy profiles (in kcal/mol) for the reactions in Figures 4–6 are presented in Figure 7 and reveal that the barriers to reaction (e.g., from the reactant complexes to their respective transition state) become substantially smaller as the number of H$_2$O molecules in the reaction system increases. This indicates water catalyzes these reactions. The reaction barrier decreases from 10.8 kcal/mol for n = 1 to 2.5 kcal/mol for n = 3 for the isobromoform + nH$_2$O → CHBr$_2$OH + HBr + (n − 1)H$_2$O reaction, from 17.6 kcal/mol for n = 1 to 2.25 kcal/mol for n = 3 for the CHBr$_2$OH + nH$_2$O → HBrCO + HBr + nH$_2$O reaction, and from 17.8 kcal/mol for n = 1 to 8.6 kcal/mol for n = 3 for the HBrCO + nH$_2$O → CO + HBr + nH$_2$O reaction.

It is instructive to compare the ab initio results to those recently found for the dissociation of HBr in H$_2$O complexes.[58-61] The stabilization of the HBr(H$_2$O)$_n$ clusters varied from 4.2 kcal/mol for n = 1 to 54.7 kcal/mol for n = 5.[60] This trend in the stabilization energies as the number of H$_2$O molecules increases is similar to that previously found for X$^-$(H$_2$O)$_n$ clusters[62,63] and the results presented here for isobromoform(H$_2$O)$_n$, CHBr$_2$-OH(H$_2$O)$_n$, and HBrCO(H$_2$O)$_n$ reactant complexes and transition states (see structures shown in Figures 4–6 and energy profiles in Figure 7). The HBr elimination reactions of the [CHBr$_2$OH]-(H$_2$O)$_n$ and [HBrCO](H$_2$O)$_n$ species are similar to the dissociation of HBr in HBr(H$_2$O)$_n$ clusters. The structures for the [CHBr$_2$OH](H$_2$O)$_n$ where n = 0,1,2,3 product complexes shows that (PC)$_4$ with no H$_2$O and (PC)$_5$ with one H$_2$O (see structures in Figure 4) have Br···H distances of 1.442 and 1.473 Å that are close to the values of 1.4–1.5 Å for a nondissociated HBr molecule in the HBr(H$_2$O)$_n$ complexes where n = 0,1,2.[60] The

(58) Conley, C.; Tao, F. M. *Chem. Phys. Lett.* **1999**, *301*, 29–36.
(59) Gertner, B. J.; Peslherbe, G. H.; Hynes, J. T. *Isr. J. Chem.* **1999**, *39*, 273–281.
(60) Cabaleiro-Lago, E. M.; Hermida-Ramón, J. M.; Rodríguez-Otero, J. *J. Chem. Phys.* **2002**, *117*, 3160–3168.
(61) Hurley, S. M.; Dermota, T. E.; Hydutsky, D. P.; Castleman, A. W., Jr. *Science* **2002**, *298*, 202–204.
(62) Lee, H. M.; Kim, K. S. *J. Chem. Phys.* **2001**, *114*, 4461–4471.
(63) Kowal, M.; Gora, R. W.; Roszak, S.; Lexczynski, J. *J. Chem. Phys.* **2001**, *115*, 9260–9265.
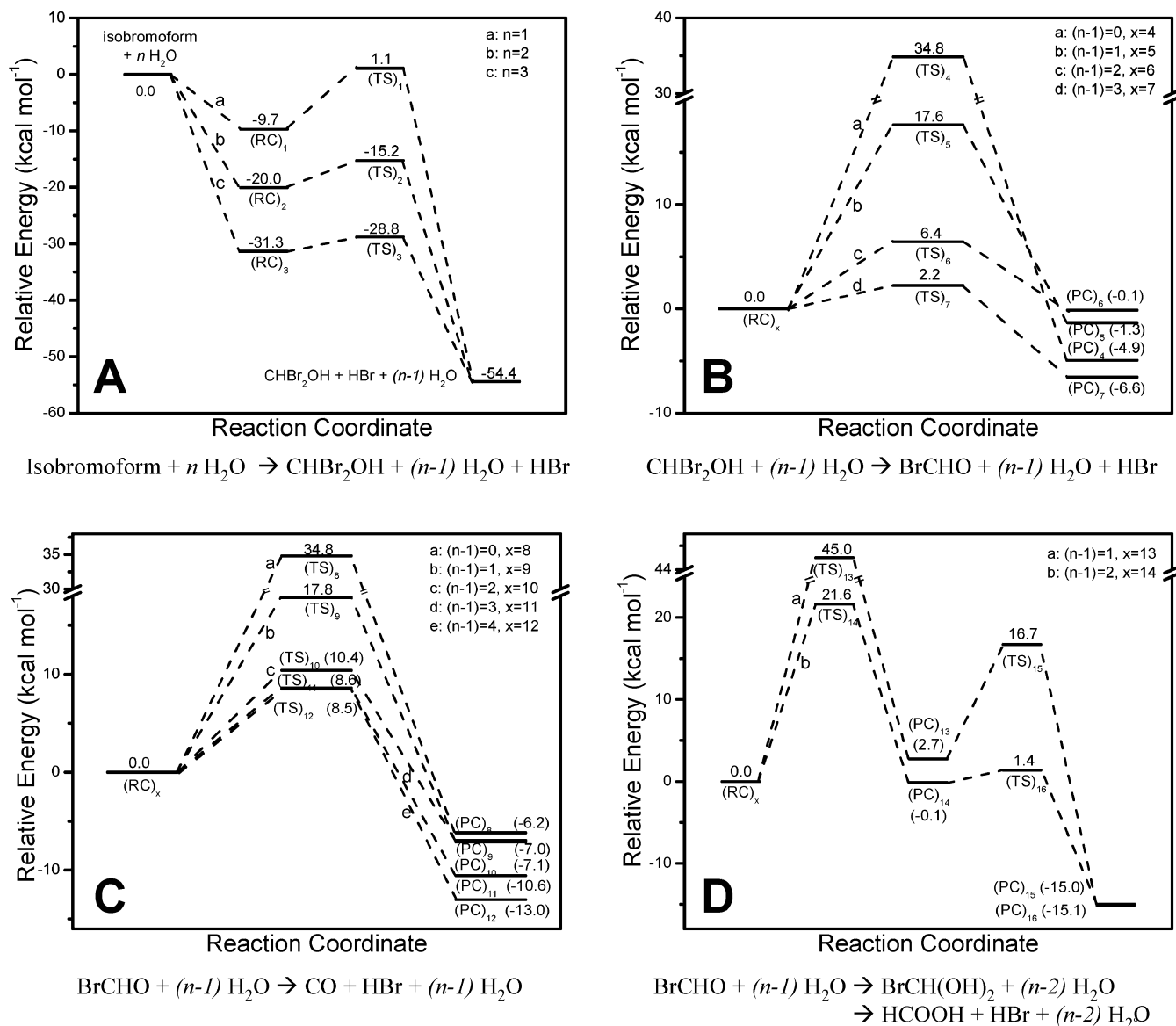
Figure 7. Relative energy profiles (in kcal/mol) obtained from MP2/6-31G* ab initio calculations to study the (A) isobromoform + $nH_2O \rightarrow CHBr_2OH$ + HBr + $(n − 1)H_2O$, where $n = 1,2,3$ with associated structures $(RC)_1–(RC)_3$, $(TS)_1–(TS)_3$, and $(PC)_1–(PC)_3$; (B) $CHBr_2OH + (n − 1)H_2O \rightarrow HBrCO$ + HBr + $(n − 1)H_2O$, where $n = 0,1,2,3$ with associated structures $(RC)_4–(RC)_7$, $(TS)_4–(TS)_7$, and PC4–PC7; and (C) HBrCO + $(n − 1)H_2O \rightarrow CO$ + HBr + $(n − 1)H_2O$, where $n = 0,1,2,3,4$ reactions with associated structures $(RC)_8–(RC)_{12}$, $(TS)_8–(TS)_{12}$, and $(PC)_8–(PC)_{12}$. Results are also shown from similar calculations for the (D) HBrCO + $(n − 1)H_2O \rightarrow HBrCOH_2$ + $(n − 2)H_2O$, where $n = 1,2,3$ with associated structures $(RC)_{13}$, $(RC)_{14}$, $(TS)_{13}$, $(TS)_{14}$, $(PC)_{13}$, and $(PC)_{14}$, and $HBrCOH_2 + (n − 2)H_2O \rightarrow HCOOH$ + HBr + $(n − 2)H_2O$, where $n = 0,1,2$ with associated structures $(RC)_{15}$, $(RC)_{16}$, $(TS)_{15}$, $(TS)_{16}$, $(PC)_{15}$, and $(PC)_{16}$, reactions. RC = reactant complex, TS = transition state, and PC = product complex.

$[CHBr_2OH](H_2O)_n$ where $n = 2,3$ product complexes (see structure $(PC)_7$ for $n = 3$ in Figure 5 as an example) have Br···H distances of 1.920 and 1.986 Å, respectively, that are closer to the values of ∼2.2 Å for a dissociated HBr molecule in the $HBr(H_2O)_n$ complexes[60] where $n = 4,5$ and suggest that HBr is mostly dissociated in the $[CHBr_2OH](H_2O)_n$ with $n = 2,3$ complexes. Similar behavior is found for the $[HBrCO](H_2O)_n$ product complexes where the H···Br distances are 1.465 and 1.521 Å, respectively, for the $n = 0$ and $n = 1$ complexes (see the structure for $(PC)_9$ for $n = 1$ as an example in Figure 5) consistent with nondissociated HBr and change to 2.136 and 2.246 Å, respectively, for the $n = 2$ and $n = 3$ complexes (see structure for $(PC)_{11}$ for $n = 3$ as an example in Figure 5) consistent with an almost complete dissociation of HBr into H_3O^+ and $Br^−$ species. These results indicate addition of more water molecules results in greater stabilization energy, lower

reaction barriers from the reactant complexes to their respective transition state, and greater dissociation of the HBr leaving group in the product complexes.

We have done an NBO analysis to find the charge on the leaving group Br atom for the reactant complexes, transition states, and product complexes involved in the reactions investigated here in Figures 4−7. The NBO charges on the leaving group Br atom in the product complexes $(PC)_4$ and $(PC)_5$ are −0.239 and −0.309, respectively, while those of $(PC)_6$ and $(PC)_7$ are much higher with values of −0.723 and −0.747, respectively. This is consistent with the $(PC)_4$ with no H_2O and $(PC)_5$ with one H_2O (see structures in Figure 4) having Br···H distances of 1.442 and 1.473 Å that are close to the values of 1.4−1.5 Å for a nondissociated HBr molecule in the $HBr(H_2O)_n$ complexes where $n = 0,1,2$, while $(PC)_6$ with two H_2O molecules and $(PC)_7$ with three H_2O molecules have Br···H

distances of 1.920 and 1.986 Å, respectively, that are closer to the values of ~ 2.2 Å for a dissociated HBr molecule in the $HBr(H_2O)_n$ complexes where $n = 4,5$.[60] A similar trend is observed for the charge on the leaving group Br atom for the $[HBrCO](H_2O)_n$ product complexes $(PC)_8-(PC)_{12}$ for the $HBrCO + nH_2O \rightarrow CO + HBr + nH_2O$ where $n = 0,1,2,3,4$ HBr elimination reactions.

The terminal Br atom of isobromoform has NBO charges of -0.58, -0.62, and -0.71 for $(RC)_1-(RC)_3$, respectively, for the isobromoform $+ nH_2O \rightarrow CHBr_2OH + HBr + (n - 1)$-$H_2O$ where $n = 1,2,3$ reactions. These charges are consistent with the isobromoform species having a $CHBr_2^+ \cdots Br^-$ character with more ionic character, longer Br–Br bond lengths, and greater stabilization energy as the number of H_2O molecules increase. The charges on the terminal Br atom increase significantly as the reactant complexes proceed to their respective transition states and have values of -0.806 for $(TS)_1$, -0.822 for $(TS)_2$, and -0.760 for $(TS)_3$. The charges initially on the leaving group Br atom of the $CHBr_2(OH)$ molecule for the $CHBr_2OH + nH_2O \rightarrow HBrCO + HBr + nH_2O$ where $n = 0,1,2,3$ reactions are fairly small for their reactant complexes with values of -0.013 for $(RC)_4$, -0.061 for $(RC)_5$, -0.085 for $(RC)_6$, and -0.121 for $(RC)_7$ [consistent with the $CHBr_2$-(OH) molecule having mostly covalent character] but increase substantially in their respective transition states to -0.710 for $(TS)_4$, -0.596 for $(TS)_5$, -0.412 for $(TS)_6$, and -0.356 for $(TS)_7$. Similarly, the charges on the Br atom of the HBrCO molecule in the $HBrCO + nH_2O \rightarrow CO + HBr + nH_2O$ where $n = 0,1,2,3,4$ reactions are moderate for their reactant complexes with values of -0.075 for $(RC)_8$, -0.157 for $(RC)_9$, -0.214 for $(RC)_{10}$, -0.200 for $(RC)_{11}$, and -0.205 for $(RC)_{12}$ and increase significantly in their respective transition states to -0.638 for $(TS)_8$, -0.696 for $(TS)_9$, -0.700 for $(TS)_{10}$, -0.688 for $(TS)_{11}$, and -0.678 for $(TS)_{12}$. For all of these reactions, the negative charge on the leaving Br atom increases significantly from the reactant complexes to their respective transition states, and as the number of H_2O molecules increases there tends to be less change in the negative charge of the leaving Br atom as the reaction goes from its reactant complex to its transition state. For example, the charges change by -0.226 from $(RC)_1$ to $(TS)_1$, -0.201 from $(RC)_2$ to $(TS)_2$, -0.053 from $(RC)_3$ to $(TS)_3$ for the isobromoform $+ nH_2O \rightarrow CHBr_2OH + HBr + (n - 1)H_2O$ where $n = 1,2,3$ O–H insertion/HBr elimination reactions. Similarly, the charges change by -0.696 from $(RC)_4$ to $(TS)_4$, -0.535 from $(RC)_5$ to $(TS)_5$, -0.327 from $(RC)_6$ to $(TS)_6$, -0.235 from $(RC)_7$ to $(TS)_7$ for the $CHBr_2OH + nH_2O \rightarrow HBrCO + HBr + nH_2O$ where $n = 0,1,2,3$ HBr elimination reactions and by -0.563 from $(RC)_8$ to $(TS)_8$, -0.539 from $(RC)_9$ to $(TS)_9$, -0.487 from $(RC)_{10}$ to $(TS)_{10}$, -0.489 from $(RC)_{11}$ to $(TS)_{11}$, and -0.472 from $(RC)_{12}$ to $(TS)_{12}$ for the $HBrCO + nH_2O \rightarrow CO + HBr + nH_2O$ where $n = 0,1,2,3,4$ HBr elimination reactions. These smaller changes in the charge distribution on the Br leaving atom as the number of water molecules increases suggest less energy is needed for redistribution of the charge to the leaving group as the reaction proceeds from the reactant complex to its corresponding transition state. This also roughly correlates with generally smaller structural changes taking place and lower reaction barrier heights (e.g., from reactant complex to transition state) as the number of H_2O

molecules increases in these reactions (see Figures 4–6). These trends are consistent with water-catalysis of these reactions.

There are some interesting differences between the dissociation of HBr in $HBr(H_2O)_n$ and the $[CHBr_2OH](H_2O)_n$ and $[HBrCO](H_2O)_n$ water-catalyzed HBr elimination reactions. For example, the proton is transferred from the HBr molecule to the O atom of a H_2O molecule in the dissociation of HBr in the $HBr(H_2O)_n$ complexes, while the proton is transferred from the OH group of the $CHBr_2OH$ molecule and the H–C moiety in the $[CHBr_2OH](H_2O)_n$ and $[HBrCO](H_2O)_n$ HBr water-catalyzed elimination reaction, respectively. This leads to the proton on the O–H group of $CHBr_2OH$ being shared with a H_2O molecule in the transition states (see structures for $(TS)_5$ and $(TS)_7$ as examples in Figures 4 and 5) of the $[CHBr_2OH](H_2O)_n$ HBr elimination reactions for $n = 1,2,3$ with the $O \cdots H-O-C$ moiety having all of the O–H distances in a narrow range (from 1.03 to 1.3 Å). Similar behavior is observed in the transition states (see structures for $(TS)_9$ and $(TS)_{11}$ as examples in Figure 5) for the $[HBrCO](H_2O)_n$ water-catalyzed HBr elimination reactions where the O–H distances in the $O \cdots H \cdots C-O$ moiety are similar to one another within a narrow range of 1.2–1.35 Å consistent with the proton being shared by a water molecule and the CO group of HBrCO. The HBr elimination process in the $[isobromoform](H_2O)_n$ is coupled to the O–H insertion reaction with water, and this results in the C–O bond formation of the H_2O molecule being coupled to a proton transfer to another H_2O molecule and the solvation of the terminal Br atom (see structures $(RC)_3$, $(TS)_3$, and $(PC)_3$ in Figure 4 for the $[isobromoform](H_2O)_3$ reaction as an example). This indicates that the water-catalyzed solvation and dissociation of a HBr or similar leaving groups may be coupled to help drive other reactions for other potential applications.

Discussion

Reaction Mechanism for the $CHBr_3 + h\nu + n(H_2O) \rightarrow CO + 3HBr + (n - 1)H_2O$ Major Product Overall Reaction. On the basis of the present experimental and theoretical results as well as other work already available in the literature, the following reaction mechanism is proposed for the $CHBr_3 + h\nu + n(H_2O) \rightarrow CO + 3HBr + (n - 1)H_2O$ major product overall reaction observed upon photolysis of low concentrations of $CHBr_3$ in aqueous solutions:

photolysis of $CHBr_3$ to form $CHBr_2$ and Br fragments

step 1 $CHBr_3 + h\nu \rightarrow CHBr_2 + Br$
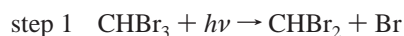
solvent-induced geminate recombination of the $CHBr_2$ and Br fragments to form isobromoform

step 2 $CHBr_2 + Br \rightarrow$ isobromoform (BrCHBr–Br)

water-catalyzed O–H insertion/HBr elimination reaction of isobromoform with nH_2O

step 3   isobromoform $+ n(H_2O) \rightarrow$

$CHBr_2OH + HBr + (n - 1)H_2O$

water-catalyzed HBr elimination reaction of $CHBr_2OH$ with nH_2O solvent

step 4 $CHBr_2OH + n(H_2O) \rightarrow HBrCO + HBr + n(H_2O)$
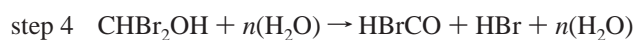
water-catalyzed HBr elimination of HBrCO in
$$n\text{H}_2\text{O solvent}$$

step 5 $\text{HBrCO} + n(\text{H}_2\text{O}) \rightarrow \text{CO} + \text{HBr} + n(\text{H}_2\text{O})$
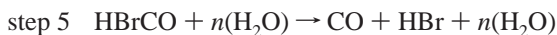
add steps 1–5 to obtain the major product overall reaction

$$\text{CHBr}_3 + h\nu + n(\text{H}_2\text{O}) \rightarrow \text{CO} + 3\text{HBr} + (n-1)\text{H}_2\text{O}$$
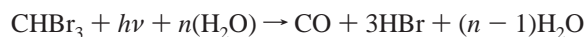
Ultraviolet excitation at wavelengths longer than 250 nm for many bromine- and/or iodine-containing polyhalomethanes in gas and solution phases results in direct cleavage of a carbon–halogen bond to produce haloalkyl radical and halogen atom fragments. A study of bromoform photodissociation in the gas phase indicated only primary C–Br bond cleavage will take place at wavelengths longer than 218 nm because there is not enough energy for secondary dissociation of the CHBr_2 radical to occur.[27] This indicates step 1 in the above reaction mechanism is the primary photochemical start of the bromoform photodissociation reaction after 240 nm excitation. Ps-TR³ experiments (see Figures S1–S5 in the Supporting Information) clearly showed that some of the initially produced CHBr_2 radical and Br atom fragments undergo solvent-induced geminate recombination to form an isobromoform species within a few picoseconds in room-temperature solutions as has been found for photolysis of other polyhalomethanes in room-temperature solutions.[32,54–57,64–66] This establishes that step 2 of the proposed reaction mechanism occurs to an appreciable degree probably on the order of 50–70%. We note that at low concentrations ($<10^{-4}$ M) most of the cage escape photofragments appear to be scavenged by the other fragment from the initially dissociated molecule which gives no appreciable Br_2, Br_2^-, or Br_3^- products. However, at higher concentrations in the millimolar and higher range, the cage escape photofragments have appreciable scavenging by fragments from other dissociated and/or reacting molecules, and absorption bands become noticeable for Br_2, Br_2^-, and Br_3^- final products in the photochemistry experiments (not shown). The present ps-TR³ experiments found the isobromoform species reacts with water to directly produce the CHBr_2OH product species (see Figure 3), and this provides direct vibrational spectroscopic evidence that isobromoform undergoes O–H insertion reactions with H_2O molecules consistent with step 3 of the proposed reaction mechanism.

The ab initio results given here indicate that CHBr_2OH undergoes water-catalyzed HBr elimination to produce HBrCO and HBr products. This is consistent with step 4 in the proposed reaction mechanism and the ps-TR³ experiments here that show accelerated decomposition of CHBr_2OH with increasing water concentration (see Figure 3C and D). Not much is known about CHBr_2OH because the ps-TR³ experimental spectra are the only experimental observation of this compound to our knowledge, but the very closely related CHCl_2OH molecule was found to decay into HClCO + HCl in the gas phase and decayed much faster in aqueous solvent (<20 μs).[67,68] The closely related

chloromethanol species has been observed in both low-temperature matrix isolation experiments[69] and gas-phase experiments[67,70] and in all cases was found to decompose in the dark to H_2CO and HCl products and to be accelerated by heterogeneous processes in the gas phase.[67] These experimental results are consistent with step 4 of the major channel proposed reaction mechanism and the current ab initio results for the HBr elimination reaction of CHBr_2OH insofar as CHBr_2OH behaves like CHCl_2OH and CH_2ClOH. Both HBrCO and HClCO were observed to decompose to CO + HX (X = Br or Cl) in the dark with the decomposition accelerated by heterogeneous processes.[68,71] In addition, the decomposition of the closely related HClCO molecule has been experimentally observed in aqueous solutions[68] and found to produce CO + HCl major products as well but at a much faster rate than in the gas-phase reaction.[71] This is consistent with step 5 of the proposed reaction mechanism and our present ab initio results for the HBrCO + $n(\text{H}_2\text{O})$ reactions. The decomposition of HClCO in aqueous solutions also formed HCOOH + HCl minor products[68] similar to the HCOOH + HBr we observe as minor products after 240 nm photolysis of CHBr_3 in water. This suggests that decomposition of HBrCO has two pathways with the major one leading to CO + HBr products in step 5 of the major reaction pathway and a minor pathway leading to HCOOH + HBr products. Further ab initio calculations were done for the HBrCO + $n(\text{H}_2\text{O}) \rightarrow \text{HBrC(OH)}_2 + (n-1)\text{H}_2\text{O}$ where $n = 1,2,3$ and the $\text{HBrC(OH)}_2 + n(\text{H}_2\text{O}) \rightarrow \text{HCOOH} + \text{HBr} + n(\text{H}_2\text{O})$ where $n = 0,1$ reactions (see structures and energy profiles in Figures 6 and 7, respectively). The barrier for the HBrCO + $n(\text{H}_2\text{O}) \rightarrow \text{HBrC(OH)}_2 + (n-1)\text{H}_2\text{O}$ where $n = 1,2,3$ reaction remains high (21.6 kcal/mol for two water molecules involved) because it is an O–H insertion reaction without an HX leaving group and is thus not significantly water-catalyzed by additional H_2O molecules beyond $n = 2$. However, the decomposition of the $\text{HBrC(OH)}_2 + n(\text{H}_2\text{O}) \rightarrow \text{HCOOH} + \text{HBr} + n(\text{H}_2\text{O})$ where $n = 0,1,2$ reaction proceeds easily (1.4 kcal/mol for one water molecule involved) as do the other HBr elimination water-catalyzed reactions of halomethanols. The high barrier for the HBrCO + $n\text{H}_2\text{O} \rightarrow \text{HBrC(OH)}_2 + (n-1)\text{H}_2\text{O}$ where $n = 1,2,3$ O–H insertion reaction (>20 kcal/mol) as compared to the low barrier for the HBrCO + $n(\text{H}_2\text{O}) \rightarrow \text{CO} + \text{HBr} + n\text{H}_2\text{O}$ where $n = 0,1,2,3$ HBr elimination reaction (about 8–9 kcal/mol) together with the proposed reaction mechanism explains why the major products are CO and 3HBr and the minor products are HCOOH and 3HBr following 240 nm photolysis of CHBr_3 in water.

Implications for Decomposition of Polyhalomethanes, Halomethanols, and Haloformaldehydes in Aqueous Environments. The ultraviolet photolysis for wavelengths >250 nm of most polyhalomethanes in the gas phase leads predominantly to a direct carbon–halogen bond cleavage and formation of haloalkyl radical and halogen atom fragments with a near unity photon quantum yield. However, ultraviolet photolysis of CHBr_3 at low concentrations in aqueous solution leads to conversion of the parent molecule into 3HBr and CO (major) and HCOOH

(64) Tarnovsky, A. N.; Alvarez, J.-L.; Yartsev, A. P.; Sündstrom, V.; Åkesson, E. *Chem. Phys. Lett.* **1999**, *312*, 121–130.
(65) Tarnovsky, A. N.; Wall, M.; Gustafson, M.; Lascoux, N.; Sündstrom, V.; Åkesson, E. *J. Phys. Chem. A* **2002**, *106*, 5999–6005.
(66) Wall, M.; Tarnovsky, A. N.; Pascher, T.; Sündstrom, V.; Åkesson, E. *J. Phys. Chem. A* **2003**, *107*, 211–217.
(67) Wallington, T. J.; Schneider, W. F.; Barnes, I.; Becker, K. H.; Sehested, J.; Nielsen, O. J. *Chem. Phys. Lett.* **2000**, *322*, 97–102.
(68) Dowideit, P.; Mertens, R.; von Sontag, C. *J. Am. Chem. Soc.* **1996**, *118*, 11288–11292.

(69) Knuttu, H.; Dahlqvist, M.; Murto, J.; Räsänen, M. *J. Phys. Chem.* **1988**, *92*, 1495–1502.
(70) Tyndall, G. S.; Wallington, T. J.; Hurley, M. D.; Scheider, W. F. *J. Phys. Chem.* **1993**, *97*, 1576–1582.
(71) Yarwood, G.; Niki, H.; Maker, P. D. *J. Phys. Chem.* **1991**, *95*, 4773–4777.

(minor) stable products with about a 0.46 photon quantum yield. These results indicate the photochemistry of $CHBr_3$ exhibits significant phase dependence with very different reactions taking place in a solvated water environment as compared to the gas phase. The water-catalyzed reactions of isobromoform with water and the subsequent HBr elimination reactions of $CHBr_2$-OH and HBrCO with water elucidated here may be noticeable sources of halogens and/or acid formation in the natural environment. To our knowledge, the water-catalyzed reactions of isopolyhalomethanes such as isobromoform have not been considered for the water-solvated photochemistry of polyhalomethanes (such as CH_2I_2, CH_2BrI, CH_2Br_2, $CHBr_3$, CCl_4, CCl_3F, and others) that have been observed in the natural environment from natural and/or man-made sources.[1−11]

The present study suggests that ultraviolet photolysis of polyhalomethanes in solvated aqueous environments would release the halogens as HX leaving groups instead of X atoms as are typically found in the gas phase. This suggests that the pH in the solvated aqueous environment around the parent polyhalomethane becomes more acidic and may significantly influence reactions associated with the activation of halogens in aqueous sea-salt particles because many reaction schemes presented depend on pH.[12−22] For halogen activation on aqueous sea salt particles, reactions such as $HOX + H^+ + X^- \rightarrow X_2 + H_2O$ (where X = Cl and/or Br) and/or $HOX^- + H^+ \rightarrow X + H_2O$ have been proposed as the key activation step where H^+ and X^- help activate the halogen atom.[12−22] The work described here indicates photolysis of $CHBr_3$ at low concentrations in a water-solvated environment releases three HBr groups. We speculate that if this happens in aqueous sea-salt particles the HBr released may cause analogous reactions to activate halogens such as by the $HOX + H^+ + Br^- \rightarrow XBr + H_2O$ reaction. Ultraviolet photolysis of several polyhalomethanes in aqueous solutions has been observed to release strong acids via their isopolyhalomethane chemistry (this work and ref 53). We note that a wide range of isopolyhalomethanes have been experimentally observed in condensed phase environments following ultraviolet photolysis of polyhalomethanes that contain Cl, Br, and/or I atoms in organic solvents.[32−34,37,39,40,55−57,64−66,72−78] This and the similar observation of isopolyhalomethanes formed in largely aqueous solutions[32] suggest that ultraviolet photolysis of many polyhalomethanes in water-solvated environments probably produces isopolyhalomethanes via solvent-induced geminate recombination of the initially formed photofragments. Thus, the formation of isopolyhalomethanes and their associated chemistry may be fairly common for polyhalomethane photochemistry in water-solvated environments. We think it would be worthwhile for a number of research groups with differing areas of expertise to pursue further research to better understand how this water-solvated chemistry may actually influence or affect the chemistry of the natural environment particularly for

reactions that are acid catalyzed in heterogeneous and/or multiphase environments.

Using the Dissociation Reaction of HX into H^+ and X^- To Drive Other Reactions. The dissociation reaction of the HBr leaving group by water into H^+ and Br^- ions helps drive several O−H insertion and HBr elimination reactions (see reaction steps 3−5 in the reaction mechanism section) that lead to formation of three Br^- ions following ultraviolet photolysis of $CHBr_3$ in water (this work and ref 24). The water solvation of the HBr leaving group enables this HX dissociation reaction into ions to be coupled to other reactions and to facilitate cleavage of C−X, O−H, and C−H bonds. For example, the water solvation of HBr helps cleave the Br−Br bond of isobromoform and an O−H bond of water during the O−H insertion reaction to make a $CHBr_2OH$ product with H_3O^+ and Br^- leaving groups (e.g., the water-solvated dissociated form of HBr). Similarly, the water solvation of HBr helps break the C−Br and O−H bonds of $CHBr_2OH$ to make a HBrCO product with H_3O^+ and Br^- leaving groups. The water solvation of HBr enables the C−H and C−Br bonds of HBrCO to be broken easily to form CO and HBr major products. This water-catalysis by solvation of a leaving group to enable its dissociation into ions (e.g., H^+ and Br^- in the example studied here) appears to be a fairly general phenomena for the dehalogenation of halogenated species in aqueous solutions. This may be utilized for improving the design and efficiency of photocatalysts and/or catalysts for decomposition of halogenated compounds in water treatment processes. The water-catalysis by solvation of a leaving group to enable its dissociation into ions helps explain where the energy comes from to break all three C−Br bonds in $CHBr_3$ to form $3Br^-$ ions. Even though excitation by one photon of ultraviolet light (240 or 253.7 nm) has only enough energy to break one C−Br bond in $CHBr_3$, this allows appreciable formation of the very reactive isobromoform species that can then undergo the water-catalyzed O−H insertion and HBr elimination reactions discussed earlier. This type of reaction can likely be even more general insofar as water solvation of a molecular leaving group leads to its dissociation into ions and can be coupled to drive other reactions. This may occur for a wide range of chemical reactions in water environments.

Conclusions

An experimental and theoretical study of the photochemistry of $CHBr_3$ in pure water and in acetonitrile/water mixed solvents was presented. Ultraviolet excitation of $CHBr_3$ in water gave almost complete conversion into 3HBr leaving groups and CO (major product) and HCOOH (minor product) molecules. Ps-TR^3 experiments in conjunction with results from ab initio calculations indicate that the water-catalyzed O−H insertion/HBr elimination reaction of isobromoform and subsequent reactions of its products lead to the production of the final products. These results have important ramifications for the phase-dependent behavior of polyhalomethane photochemistry and chemistry in water-solvated environments relative to gas-phase reactions. Gas-phase photolysis with ultraviolet light (>230 nm) of polyhalomethanes typically results primarily in cleavage of one carbon−halogen bond to produce a haloalkyl radical and halogen atom fragments. In contrast, ultraviolet photolysis (>230 nm) of polyhalomethanes such as $CHBr_3$ at low concentrations in water-solvated environments appears to lead to cleavage of multiple carbon−halogen bonds and releases

(72) Maier, G.; Reisenauer, H. P. *Angew. Chem., Int. Ed. Engl.* **1986**, *25*, 819−822.
(73) Maier, G.; Reisenauer, H. P.; Hu, J.; Schaad, L. J.; Hess, B. A., Jr. *J. Am. Chem. Soc.* **1990**, *112*, 5117−5122.
(74) Tarnovsky, A. N.; Wall, M.; Rasmusson, M.; Pascher, T.; Åkesson, E. *J. Chin. Chem. Soc.* **2000**, *47*, 769−772.
(75) Zheng, X.; Phillips, D. L. *Chem. Phys. Lett.* **2000**, *324*, 175−182.
(76) Zheng, X.; Phillips, D. L. *J. Phys. Chem. A* **2000**, *104*, 6880−6886.
(77) Zheng, X.; Phillips, D. L. *J. Chem. Phys.* **2000**, *113*, 3194−3203.
(78) Zheng, X.; Kwok, W. M.; Phillips, D. L. *J. Phys. Chem. A* **2000**, *104*, 10464−10470.

halide ions as part of strong acid leaving groups. The solvation of the HBr leaving group by water enables the dissociation reaction into H^+ and Br^- ions to be used to catalyze several O−H insertion and HBr elimination reactions of isobromoform and its reaction products. This enables O−H and C−H bonds to be cleaved more easily in the presence of water molecules than in the absence of water molecules.

Supporting Information Available: Details for finding the experimental estimate of the photoquantum yield for formation of $3Br^-$ from ultraviolet photolysis of $CHBr_3$ in water, Figures S1−S5 showing an overview of the ps-TR^3 spectra obtained at varying time delays following 267 nm photolysis of $CHBr_3$ in acetonitrile/trace amounts, 0.2%, 1%, 2%, and 5% water mixed solvents, and Table S1 comparing the isobromoform Raman band vibrational frequencies obtained in this work to those previously obtained in cyclohexane solution and from density functional theory calculations of ref 31. Cartesian coordinates, total energies, and zero-point energies obtained from the ab initio calculations (PDF). This material is available free of charge via the Internet at http://pubs.acs.org.

JA0390552